

## Tahiti: Geochemical evolution of a French Polynesian volcano

Robert A. Duncan and Martin R. Fisk

College of Oceanic and Atmospheric Sciences, Oregon State University, Corvallis

William M. White

Department of Geological Sciences, Cornell University, Ithaca, New York

Roger L. Nielsen

College of Oceanic and Atmospheric Sciences, Oregon State University, Corvallis

**Abstract.** The island of Tahiti, the largest in French Polynesia, comprises two major volcanoes aligned NW-SE, parallel with the general trend of the Society Islands hotspot track. Rocks from this volcanic system are basalts transitional to tholeiites, alkali basalts, basanites, picrites, and evolved lavas. Through K-Ar radiometric dating we have established the age of volcanic activity. The oldest lavas (~1.7 Ma) crop out in deeply eroded valleys in the center of the NW volcano (Tahiti Nui), while the main exposed shield phase erupted between 1.3 and 0.6 Ma, and a late-stage, valley-filling phase occurred between 0.7 and 0.3 Ma. The SW volcano (Tahiti Iti) was active between 0.9 and 0.3 Ma. There is a clear change in the composition of lavas through time. The earliest lavas are moderately high SiO<sub>2</sub>, evolved basalts (Mg number (Mg# = Mg/Mg+Fe<sup>2+</sup>) 42-49), probably derived from parental liquids of composition transitional between those of tholeiites and alkali basalts. The main shield lavas are predominantly more primitive olivine and clinopyroxene-phyric alkali basalts (Mg# 60-64), while the later valley-filling lavas are basanitic (Mg# 64-68) and commonly contain peridotitic xenoliths (olivine+orthopyroxene+clinopyroxene+ spinel). Isotopic compositions also change systematically with time to more depleted signatures. Rare earth element patterns and incompatible element ratios, however, show no systematic variation with time. We focused on a particularly well exposed sequence of shield-building lavas in the Punaruu Valley, on the western side of Tahiti Nui. Combined K-Ar ages and magnetostratigraphic boundaries allow high-resolution age assignments to this ~0.7-km-thick flow section. We identified an early period of intense volcanic activity, from 1.3 to 0.9 Ma, followed by a period of more intermittent activity, from 0.9 to 0.6 Ma. Flow accumulation rates dropped by a factor of 4 at about 0.9 Ma. This change in rate of magma supply corresponds to a shift in activity to Tahiti Iti. We calculated the composition of the parent magma for the shield-building stage of volcanism, assuming that it was in equilibrium with Fo<sub>89</sub> olivine and that the most primitive aphyric lavas were derived from this parent by the crystallization of olivine alone. The majority of the shield lavas represent 25 to 50% crystallization of this parent magma, but the most evolved lavas represent about 70% crystallization. From over 50 analyzed flow units we recognize a quasi-periodic evolution of lava compositions within the early, robust period of volcanic activity, which we interpret as regular recharge of the magma chamber (approximately every 25 ± 10 kyr). Volcanic evolution on Tahiti is similar to the classic Hawaiian pattern. As the shield-building stage waned, the lavas became more silica undersaturated and isotopic ratios of the lavas became more MORB-like. We propose that the Society plume is radially zoned due to entrainment of a sheath of viscously coupled, depleted mantle surrounding a central core of deeper mantle material. All parts of the rising plume melt, but the thermal and compositional radial gradient ensures that greater proportions of melting occur over the plume center than its margins. The changing composition of Tahitian magmas results from lithospheric motion over this zoned plume. Magmas erupted during the main shield-building stage are derived mainly from the hot, incompatible element-enriched central zone of the plume; late-stage magmas are derived from the cooler, incompatible element-depleted, viscously coupled sheath. A correlation between Pb/Ce and isotope ratios suggests that the Society plume contains deeply recycled continental material.

### Introduction

Linear chains of volcanic islands and seamounts are a conspicuous feature of the Pacific Ocean floor, especially its

south central region known as French Polynesia. Here, several separate, subparallel island chains strike west-northwest, aligned in the direction of Pacific plate motion. Young to active volcanism occurs at the southeast end of each of these groups. It is now generally accepted that such volcanic lineaments are the consequence of plate motion over long-lived hotspots, which are proposed to be sublithospheric thermal anomalies maintained by rising convective plumes of deeper mantle material [Morgan, 1971, 1972].

Copyright 1994 by the American Geophysical Union.

Paper number 94JB00991.  
0148-0227/94/94JB-00991\$05.00

Hotspot-related oceanic islands are also significant as geochemical records of mantle-lithosphere interaction, mantle melting and magma transport processes, and the temporal and spatial scales of mantle heterogeneity. In contrast to the first-order uniformity of compositions of mid-ocean ridge basalts (MORBs), ocean island basalts (OIBs) show tremendous variability. The compositional range of volcanic products in French Polynesia reflects melt contributions from several mantle reservoirs that have remained isolated from one another for periods appropriate to mixing times for whole mantle convection [Gurnis and Davies, 1986]. The origin of mantle heterogeneities may lie in melting and fractionation processes, recycling of lithosphere, metasomatism, and mantle-lithosphere assimilation. However, understanding the nature and significance of distinct sources for melt generation requires resolution of the volcanic histories of individual oceanic islands.

This paper describes the volcanic history of Tahiti, the largest island in the Society Islands chain. We begin with radiometric dating to establish the time frame of volcanic activity. Next, we present whole rock and mineral major and trace element abundances from which we infer parent magma compositions. Isotopic data are used to evaluate mantle source variability throughout the construction of Tahiti. Finally, we assess fractionation, recharge, and assimilation effects in a 700-m-thick section in the Punaruu Valley. We combine compositional variations with age determinations to estimate recharge and fractionation rates.

### Geological Setting and Previous Work

The Society Islands chain is a ~700-km lineament composed of islands, atolls, and seamounts, all of which are predominantly volcanic. Individual volcanic centers rise separately from abyssal depths of 3.5 to 4 km below sea level and were erupted onto ~60 Ma oceanic lithosphere. Previous

radiometric dating has shown that island ages become progressively older to the northwest, at a rate of 10 to 11 cm/yr [Duncan and McDougall, 1976]. The orientation of the chain and the age distribution of the volcanism are compatible with Pacific plate motion over a stationary hotspot [Duncan and Clague, 1985].

Tahiti, the largest of these islands, lies near the southeast end of the chain. This island comprises two major coalesced volcanoes, aligned NW-SE, parallel with the general trend of the Society hotspot track. Volcanic activity here ceased at about 0.2 Ma [Dymond, 1975; Duncan and McDougall, 1976; Becker et al., 1974; Gillot et al., 1993]. The present-day position of the hotspot southeast of Tahiti is indicated by the young island of Mehetia (0.0 to 0.3 Ma [Binard et al., 1993; R. Duncan, unpublished data, 1993]), intense seismic activity [Talandier and Okal, 1984], and active submarine volcanoes [Cheminee et al., 1989; Devey et al., 1990].

Tahiti is roughly 30 km wide and 55 km along the axis of the two volcanoes and has a total volume of about  $6 \times 10^4$  km<sup>3</sup>, of which about 2% lies above sea level (Figure 1). The volcanoes are composed predominantly of basaltic lava flows, but pyroclastic rocks related to localized phreatic eruptions occur in coastal outcrops, and subordinate differentiated rocks (hawaiite-mugearite-trachyte-phonolite series) are common as plugs, sills, and irregular flows [DeNeufbourg, 1965]. Remnants of the original shield ("planeze") are separated by deeply incised, radial valleys that provide spectacular topographic relief (~2 km) and offer extraordinary access to the volcanic stratigraphy. Gillot et al. [1993] reported east-west trending rift zones that cut the shield and evidence of caldera collapse at the main eruptive centers. Posterosional eruptions from these centers have partially filled old river valleys ("remplissage des vallees"). Tahiti is remarkable in displaying the most extensive suite of plutonic rocks among Pacific islands. These are found in the eroded centers of both volcanoes, having crystallized some 2 to 3 km below the original summits of the shields [Williams, 1933].

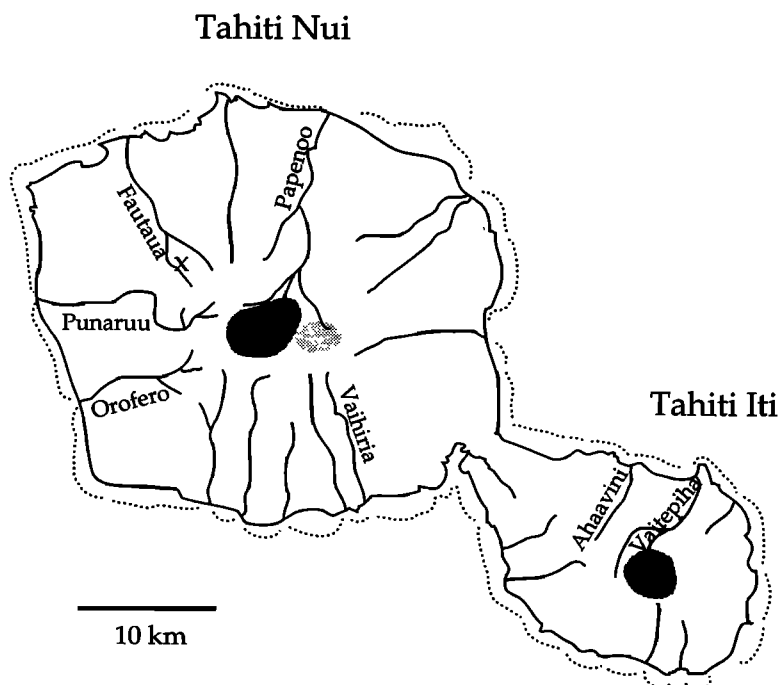


**Figure 1.** Map of Tahiti showing major features mentioned in the text. Heavy shading indicates areas of plutonic rocks. Light shading is the area of oldest central lavas. Dotted lines are fringing reefs. Sample locations (latitude, longitude, and elevation) are listed in Table A1. Cross marks a xenolith location discussed in the text.

Early geologic and petrologic studies [Lacroix, 1910; Marshall, 1915; Williams, 1933; DeNeufbourg, 1965; McBirney and Aoki, 1968] established that most Tahitian rocks are moderately evolved alkali basalts and low-pressure fractional crystallization derivatives from them. The late-stage, valley-filling lavas are relatively primitive basanitic rocks. An important aspect of these late-stage flows is that they commonly contain ultramafic xenoliths of dunite, harzburgite, wehrlite, and spinel lherzolite [Duncan, 1975; Tracy, 1980]. The plutonic rocks are chemical equivalents of alkali basalts and basanites, but most appear to be related to the posterosional volcanic phase. Lava flows from the deepest stratigraphic level exposed on the island are hypersthene-normative, high-silica basalts, transitional between alkali basalt and tholeiitic compositions [Duncan et al., 1987]. Given the predominance of tholeiitic lavas in the shield-building stage of Hawaiian Islands [Macdonald and Katsura, 1964] and the discovery of tholeiitic compositions in early lavas from the Marquesas [Duncan et al., 1986; Desonie et al., 1993] and Samoan Islands [Natland and Turner, 1985], it seems possible that submarine portions of the Society islands are also tholeiitic. However, Devey et al. [1990] found no tholeiitic basalts among dredged samples from the young seamounts southeast of Tahiti, so the nature of early volcanism at Society volcanoes remains enigmatic.

### Sampling and Field Studies

Most of the samples used in this study (prefix T85-) were collected in 1985 during a joint U.S.-French program of field measurements and sampling. Seven river canyon sections were examined to distinguish shield and valley-filling sequences. We also visited the central region of the island (Figure 1) to examine the plutonic complex and sample what turn out to be the oldest lavas on the island. Xenoliths were collected from valley-filling lavas in the Fautaua, Punaruu and Papenoo valleys. Additional samples (prefixes T73- and T74-) are from Duncan's [1975] thesis collection at the Australian National University and come primarily from the uppermost Punaruu section. Paleomagnetic cores from Punaruu Valley lava flows

(sample numbers other than T73-, T74-, and T85-) are those described by Chauvin et al. [1990].

The thick sequence of seaward dipping lava flows exposed in the Punaruu Valley (Figure 2) was erupted during the main phase of shield construction. Rapid erosion during periodic storms and active quarrying have provided fresh outcrop surfaces. Flow orientations and thicknesses were recorded to construct measured sections; dips are typically 8 to 10°, and flows are 1 to 3 m thick. Individual flows can be traced for hundreds of meters along the canyon walls. Although there are several discordances in the section due to infilling of erosional surfaces, these are relatively minor, and the gross structure is a monotonic sequence of flows (Figure 2). The 700-m-thick section is nearly entirely lava flows with rubbly tops and bottoms and blocky to columnar centers. Dikes are rare, indicating that the eruption center was distant. Valley-filling lava flows cover the inland extremity of this section. Paleomagnetic directions were determined from oriented cores after the cores had been subjected to standard magnetic cleaning methods [Chauvin et al., 1990].

### Radiometric Age Determinations

#### Timing for Tahitian Volcanism

Shield lavas, valley-filling lavas, and differentiated rocks were selected for K-Ar age determinations after petrographic examination for degree of alteration and crystallinity. Rocks were trimmed to remove any weathered surfaces, crushed and sieved to ~0.5 mm size fraction, and ultrasonically washed in distilled water. A split (~5 g) was then powdered for K analysis by atomic absorption spectrophotometry. Because xenolithic material contains mantle-derived Ar [Jager et al., 1985], porphyritic samples were avoided or hand-picked to remove olivine and pyroxene. Ar was extracted and purified from 1 to 5 g whole rock samples by radio frequency (RF) induction heating in high-vacuum glass lines with Ti getters. The isotopic composition of  $^{38}\text{Ar}$ -spiked Ar was measured using an

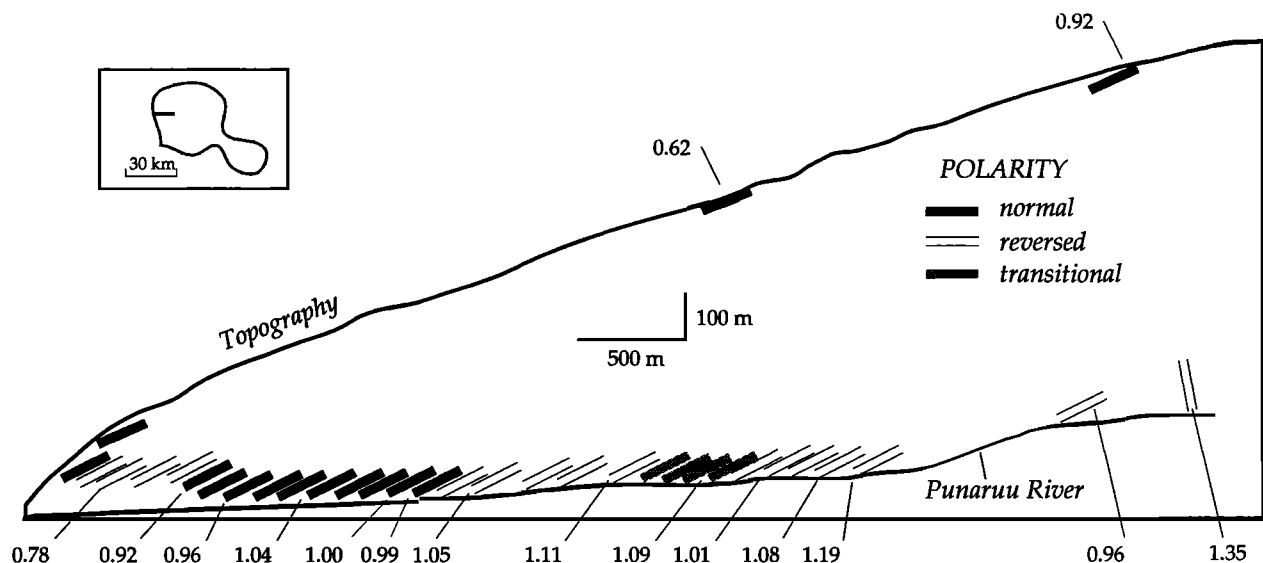


**Figure 2.** Schematic cross section of the Punaruu Valley and locations from which dated samples were collected. Average flow dips are 10°; one dike is nearly vertical, as pictured. Although shown as a simple monotonic succession of flows, the section does exhibit evidence of minor inversions of relief due to periods of erosion and valley-filling flows. Magnetostratigraphic data are from Chauvin et al. [1990]; sample ages (in millions of years) are indicated.

**Table 1.** K-Ar Age Determinations for Volcanic Rocks From Tahiti, French Polynesia

Sample	Location	%K	Radiogenic $^{40}\text{Ar}$ (rad)		Age $\pm 1\sigma$ , Ma
			( $\times 10^{-7}$ cm/g)	%	
<i>Tahiti Nui</i>					
T85-41	center, flow	1.57	0.9967	17.1	1.67 $\pm$ 0.05
T85-43	center, dike	1.81	0.5041	9.6	0.73 $\pm$ 0.03
T85-44	center, flow	1.78	0.7773	12.6	1.12 $\pm$ 0.03
T85-7	Punaruu, flow	1.32	0.4812	13.4	0.96 $\pm$ 0.04
BKV-185*	Punaruu, flow	0.83	0.3845	27.9	1.19 $\pm$ 0.02
T85-72*	Punaruu, flow	0.86	0.3529	15.2	1.08 $\pm$ 0.02
T85-76*	Punaruu, flow	1.03	0.3964	10.8	1.01 $\pm$ 0.05
BKG-85*	Punaruu, flow	2.07	0.8767	24.4	1.09 $\pm$ 0.02
PKB-14*	Punaruu, flow	1.16	0.4991	18.4	1.11 $\pm$ 0.03
T85-81*	Punaruu, flow	1.03	0.4092	24.4	1.05 $\pm$ 0.02
T85-87	Punaruu, flow	0.91	0.3526	33.1	0.99 $\pm$ 0.02
T85-93*	Punaruu, flow	1.28	0.4872	19.8	1.00 $\pm$ 0.02
T74-431*	Punaruu, flow	1.62	0.6396	17.0	1.04 $\pm$ 0.02
T74-434*	Punaruu, flow	1.16	0.4233	11.8	0.96 $\pm$ 0.02
T74-435*	Punaruu, flow	1.34	0.4701	17.8	0.92 $\pm$ 0.02
T85-61	Punaruu, flow	1.49	0.5307	3.8	0.92 $\pm$ 0.06
T74-437*	Punaruu, flow	1.66	0.4928	14.2	0.78 $\pm$ 0.01
T85-67*	Punaruu, flow	2.19	0.5296	6.6	0.62 $\pm$ 0.02
T85-19	Papenoo, flow	0.96	0.4715	2.3	1.27 $\pm$ 0.12
T85-28	Papenoo, flow	0.88	0.3710	7.9	1.09 $\pm$ 0.05
T85-34	Papenoo, flow	0.84	0.2496	4.7	0.76 $\pm$ 0.05
T85-101	Papenoo, flow	1.19	0.2225	6.0	0.49 $\pm$ 0.02
T85-102	Papenoo, flow	3.14	0.6222	4.7	0.52 $\pm$ 0.02
T85-24	Papenoo, flow	1.31	0.2630	7.4	0.52 $\pm$ 0.01
T85-25	Papenoo, flow	1.28	0.2542	1.9	0.51 $\pm$ 0.07
T85-12	Papenoo, flow	1.16	0.1678	2.6	0.37 $\pm$ 0.07
T85-33	Papenoo, flow	1.31	0.1273	2.7	0.25 $\pm$ 0.02
T85-95	Fautaua, flow	0.99	0.2991	32.4	0.78 $\pm$ 0.01
T85-96	Fautaua, flow	0.88	0.2220	1.6	0.65 $\pm$ 0.08
T85-47	Vaihiria, flow	1.57	0.5404	2.5	0.89 $\pm$ 0.07
T85-111	Vaihiria, flow	1.08	0.3445	5.3	0.82 $\pm$ 0.03
T85-103	Vaihiria, flow	1.44	0.3754	4.2	0.67 $\pm$ 0.03
<i>Tahiti Iii</i>					
T85-116	Ahaavini, cobble	3.72	0.7416	4.0	0.51 $\pm$ 0.03
T85-117	Vaitepiha, dike	1.24	0.4562	1.4	0.95 $\pm$ 0.18

Age calculations are based on the following decay and abundance constants:

$\lambda_{\text{e}} = 0.581 \times 10^{-10} \text{ yr}^{-1}$ ;  $\lambda_{\text{b}} = 4.962 \times 10^{-10} \text{ yr}^{-1}$ ;  $^{40}\text{K}/\text{K} = 1.167 \times 10^{-4} \text{ mol/mol}$ .

\*Reported initially by *Chauvin et al.* [1990].

AEI MS-10S mass spectrometer with digital data acquisition. Precise ages (typically 1-5% analytical uncertainty) were obtained for rocks as young as 0.3 Ma by virtue of relatively high sample K contents and daily monitoring of the mass fractionation of our instrument [e.g., *Levi et al.*, 1988].

New age determinations, together with some previously reported data [*Chauvin et al.*, 1990] are presented in Table 1. In general, they are compatible with earlier reported radiometric ages from Tahiti [*Becker et al.*, 1974; *Dymond*, 1975; *Duncan and McDougall*, 1976; *Leotot et al.*, 1990]. A few, much older ages [*Krummenacher and Noetzelin*, 1966; *Dymond*, 1975] from plutonic rocks are certainly not reliable crystallization ages due to excess  $^{40}\text{Ar}$  trapped during cooling. Because they are tied to the volcanic stratigraphy through outcrop sampling, the new ages place a definitive time frame on the volcanic evolution of the island.

The oldest exposed rocks are from the eroded center of the island. Few of these were fresh enough for dating; zeolites, clays and carbonate have replaced much of the groundmass and olivine phenocrysts. Two of the freshest samples, however,

gave ages of 1.67  $\pm$  0.05 and 1.12  $\pm$  0.03 Ma. Both samples produced low total oxides (~96 wt. %), indicating some replacement of igneous phases with hydrous alteration phases. This is a concern because of possible radiogenic  $^{40}\text{Ar}$  loss and/or K mobilization, both of which would disrupt the K-Ar system. The K contents of these samples, however, are concordant with overall variation of  $\text{K}_2\text{O}$  with MgO within shield lavas, and we conclude that K loss (or addition) has not been significant. Radiogenic  $^{40}\text{Ar}$  loss is probable but harder to evaluate without additional age determinations from the central section of lavas. Hence we view the 1.67 Ma age as approximate, but it is probably a minimum age given the likelihood of some Ar loss. This section is cut by a dike of basanitic composition, dated at 0.73  $\pm$  0.04 Ma, which we surmise fed valley-filling flows. The Punaruu, Papenoo, and Vaihiria canyon sequences all produced ages in the 1.3 to 0.6 Ma range, which we ascribe to the main shield-building phase. The older central lavas may sensibly be included in this phase on structural grounds but have been separated here on the basis of compositions [*Duncan et al.*, 1987; *Cheng et al.*, 1993]

(also see below). Valley-filling flows began about 0.7 Ma and continued to at least 0.25 Ma. Hence shield and valley-filling phases overlapped for a short time, at 0.6 to 0.7 Ma. Volcanic activity at Tahiti Iti was contemporaneous with that at Tahiti Nui but occurred over a shorter period, from 1.0 to 0.3 Ma [Duncan, 1975; Leotot *et al.*, 1990; this study].

### The Punaruu Valley Section

Age determinations on 16 samples from the Punaruu valley section appear in Table 1, and their locations are shown in Figure 2. The age succession is consistent with the stratigraphic order of the lava flows, with the exception of sample T85-7, which probably comes from a flow filling an old erosional depression (P.-Y. Gillot, personal communication, 1994). Additional age control is provided by flow-by-flow magnetostratigraphy [Chauvin *et al.*, 1990]. Three magnetic polarity reversals were observed in the section and correlate with the Brunhes-Matuyama, Matuyama-Jaramillo, and Jaramillo-Matuyama transitions. An apparent reversed-transitional-reversed (R-T-R) excursion was identified lower in the sequence, and K-Ar age determinations around 1.1 Ma suggest that it corresponds to the Cobb Mountain subchron. The Brunhes-Matuyama and the lower Jaramillo transitions are defined by only a few intermediate directions while many intermediate directions were observed for the upper Jaramillo transition and the Cobb Mountain excursion. These differences were attributed to variations in the rate of eruption during construction of the shield sequence.

The 700-m-thick Punaruu valley section formed between 1.3 and 0.6 Ma, yielding an average accumulation rate of 1.0 km/m.y., or approximately one flow every 2000 years. Evidence from the radiometric dating and the paleomagnetic studies, however, is that flows were erupted in pulses with significant time gaps rather than at regular intervals. This may reflect morphologic evolution of the volcano and preferential channeling of flows or may reflect changes in location of eruptive centers. The majority (80%) of the section formed between 1.3 and 0.9 Ma, indicating an early period of intense activity, followed by a period of intermittent activity between 0.9 and 0.6 Ma. Flow accumulation rates dropped by a factor of 4 between these two intervals. The timing of change in magma supply corresponds approximately with a shift in shield-building activity to Tahiti Iti and with the beginning of valley-filling volcanism at Tahiti Nui.

### Geochemistry: Methods and Results

Geochemical data in supplementary Tables A1-A4 (major and trace element concentrations and isotopic compositions) for samples analyzed here are available electronically<sup>1</sup> or as hard copies from the authors. The major element concentrations were determined by X ray fluorescence (XRF), by microprobe of fused glasses (MFG) at Oregon State University, and by direct current plasma spectroscopy (DCP) at the Lamont-Doherty Earth Observatory of Columbia University. The major element analyses are presented electronically, divided into two parts. The first half of the

table includes rocks from a number of locations from both volcanoes of Tahiti. The second half of the table includes extrusive rocks of the shield-building phase of volcanism from the Punaruu Valley, arranged in stratigraphic order.

Several laboratories contributed XRF analyses. Samples analyzed by more than one laboratory show good agreement except that a correction was needed for an interlaboratory bias of SiO<sub>2</sub> (+2.0 wt. %) between the Oregon State University analyses and those of other laboratories. Comparisons between other analytical techniques are equally favorable, except that microprobe analyses of K<sub>2</sub>O in fused glasses with high K<sub>2</sub>O (> 4 wt. %) are consistently lower than the XRF analyses of the same samples. This difference, due to the volatilization of K<sub>2</sub>O during melting of the samples, has no impact on the conclusions of this paper.

Trace element concentrations were determined by XRF, DCP, and inductively coupled plasma mass spectrometry (ICPMS) at Cornell University and are presented in Table A3. For ICPMS analyses, approximately 200 mg of sample were digested with a 4:1 HNO<sub>3</sub>-HF mixture in Savilex capsules for 48 hours. After evaporating to dryness, they were redissolved in 8 mL HNO<sub>3</sub> and diluted to 200 mL with distilled water. The solutions were then analyzed using a FISON Plasmaquad 2+ mass spectrometer equipped with a high performance interface. The analysis employed the drift-corrected external calibration technique of Cheatham *et al.* [1993]. External calibration standards were matrix matched (i.e., solutions of interlaboratory or in-house basalt standards were employed). To maximize precision and minimize residual drift errors, each sample was analyzed between 3 and 5 times. A blank and a quality control standard were analyzed with each batch of samples. Analytical uncertainty, as judged from repeated analyses of U.S. Geological Survey standard BHVO-1, ranges from 1.1% for Yb and Lu to 5.4% for Th. Accuracy has been assessed from the mean of the analyses of BHVO-1. These values are in excellent agreement with those determined at Cornell by the more precise methods of thermal ionization mass spectrometry isotope dilution and ICPMS standard addition [Cheatham *et al.*, 1993; White *et al.*, 1993].

Sr, Nd, and Pb isotopic compositions were determined for a number of samples (Table A4). Values for interlaboratory standards and estimates of analytical uncertainty based on replication of those standards are given. In addition to samples collected in 1985, we include in this table several samples obtained from the Smithsonian Institution. Most samples were analyzed on a VG Sector mass spectrometer at Cornell using methods described by White *et al.* [1990]. A few were run on a VG Sector 54 mass spectrometer at Cornell using essentially identical methods. We analyzed two samples (T85-41 and T85-19) also analyzed by Cheng *et al.* [1993]. Our Nd isotopes ratios agree well with those they reported, and our <sup>87</sup>Sr/<sup>86</sup>Sr ratio for T85-41 (after leaching) agrees exactly with the ratio they report. Our <sup>87</sup>Sr/<sup>86</sup>Sr ratio for T85-19 is about 0.00004 less than the value they report. The difference may reflect slight contamination; we leached samples before analysis, but Cheng *et al.* did not. The Pb isotope ratios we determined for T85-41 are significantly lower than the values reported by Cheng *et al.* [1993]. The difference may also reflect slight contamination that was removed by leaching in our procedure. Alternatively, it may reflect a difference in the way the fractionation correction was performed or an interlaboratory bias.

A diagram of total alkalis and silica (Figure 3) shows that the oldest rocks (central) fall within a restricted range of 4.6 to 5.8 wt. % alkalis and 48 to 49.5 wt. % SiO<sub>2</sub>. Most rocks from the shield-building stage of volcanism have lower silica and total alkalis than do the central rocks. The composition of rocks from the last stage of volcanism (valley-filling) overlaps with that of the shield-building stage but is at the low

<sup>1</sup>An electronic supplement of this material may be obtained on a diskette or Anonymous FTP from KOSMOS.AGU.ORG. (LOGIN to AGU's FTP account using ANONYMOUS as the username and GUEST as the password. Go to the right directory by typing CD APEND. Type LS to see what files are available. Type GET and the name of the file to get it. Finally, type EXIT to leave the system.) (Paper 94JB00991, Tahiti: Geochemical evolution of a French Polynesian volcano, by Robert A. Duncan *et al.*) Diskette may be ordered from American Geophysical Union, 2000 Florida Avenue, N.W., Washington, DC 20009; \$15.00. Payment must accompany order.

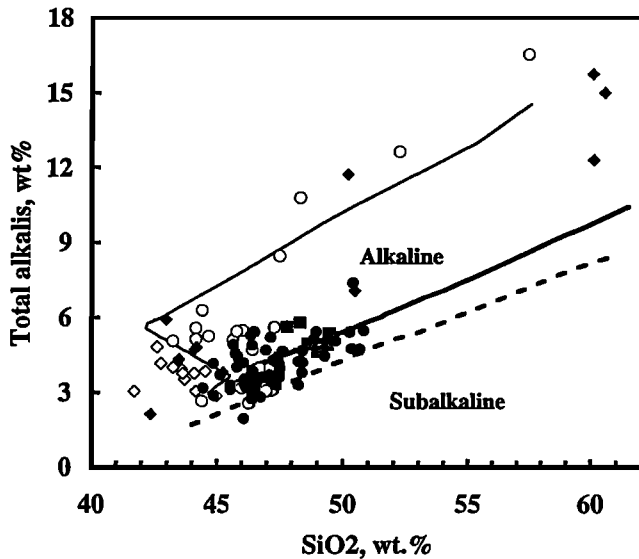


**Figure 3.** Silica-alkali diagram for volcanic rocks from Tahiti. Patterned squares are from the central area of Tahiti Nui (oldest lavas), open circles are from the shield-building phase of volcanism (intermediate age), and the open diamonds are from the valley-filling series (youngest lavas). Solid circles are from the Punaruu Valley (0.6 to 1.2 Ma). Solid diamonds are from Tahiti Iti. Dashed line separates alkaline from subalkaline magmas. Heavy solid line indicates the fractionation trend from a parental shield magma (Table 2) under relatively oxidizing conditions (two log units above the quartz-fayalite-magnetite, QFM, buffer). The light solid line shows the liquid line of descent of a magma with lower silica and under more reducing conditions (one log unit above QFM) than the shield magma.

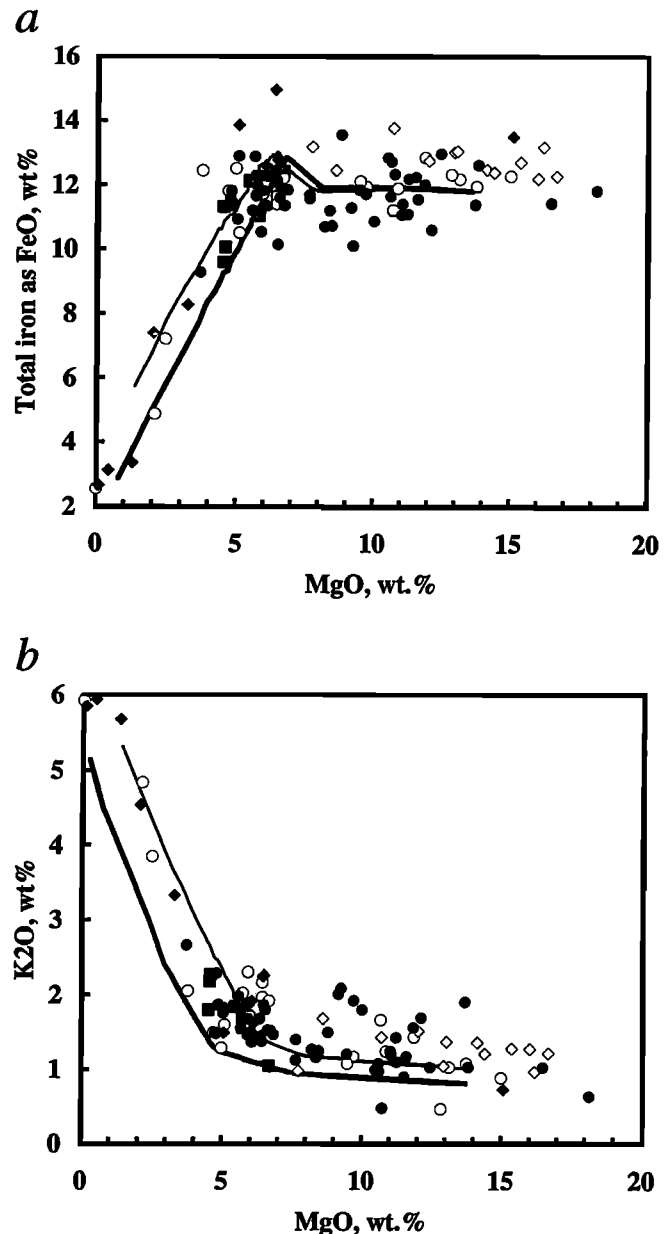
end of the  $\text{SiO}_2$  range of these lavas (Figure 3). These three groups of lavas describe a trend of decreasing silica with time, although the Punaruu Valley sequence alone covers much of the compositional range of the central, shield, and valley-filling lavas.

These relationships also exist in MgO variation diagrams (Figure 4), which show that the central lavas are more evolved than most of the shield and valley-filling lavas. The shield lavas extend to more evolved compositions than do many of the valley-filling lavas. (Here degree of evolution is indicated, to first order, by MgO abundance.) Phenocrysts in these rocks are primarily olivine and pyroxene; considerable accumulation of these phases is evident in some rocks (picrites and ankaramites).

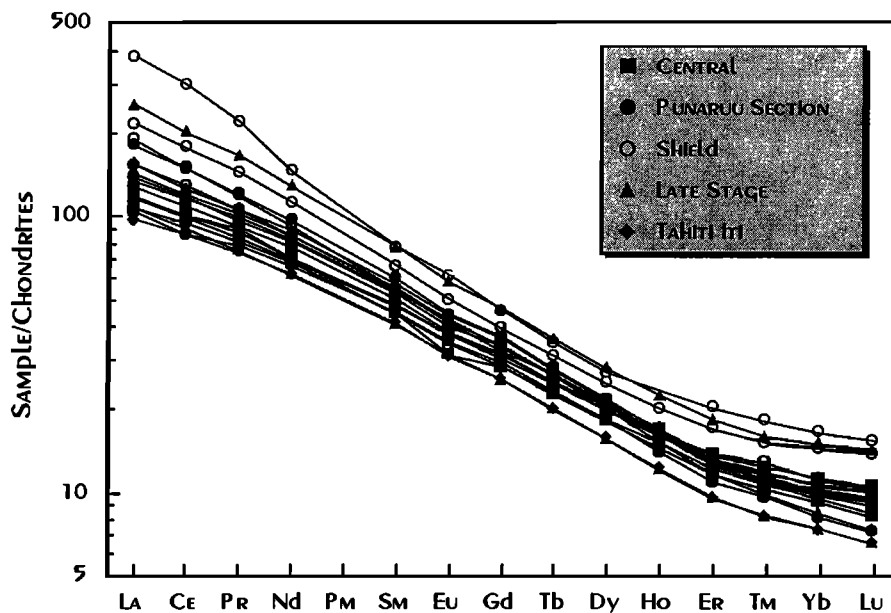
Rare earth patterns are shown in Figure 5. With the exception of T85-102, the most rare earth rich sample, the patterns are remarkably similar despite the wide variation in major element and isotopic composition of these samples. All samples are strongly light rare earth enriched and have steep middle and heavy rare earth patterns, as reported for all volcanoes in the Society hotspot lineament [Dostal *et al.*, 1982]. Assuming the heavy rare earth pattern of the source is flat or nearly so, the steep heavy rare earth pattern and the low concentrations of the heavy rare earth elements suggest that these magmas were generated in the garnet stability field. T85-102 is a mugearite whose high overall abundance of rare earths and light rare earth enrichment is undoubtedly a result of extensive fractional crystallization.

Figure 6 displays average incompatible element concentrations for central, shield, late-stage, and Tahiti Iti groups in a "spider diagram," in which elements are ordered by

increasing compatibility. All groups have similar abundances of these elements, although there are several subtle but significant differences. First, the central lavas show a negative Sr anomaly. We suspect this may reflect fractionation of plagioclase, which is an occasional phenocryst in the central lavas but not in other lavas. Second, the central lavas have a slight positive Pb anomaly. Though not large, we believe this feature is real and associated with the



**Figure 4.** MgO variation diagrams for Tahiti volcanic rocks. (a) MgO-FeO. The fractionation lines indicate the change in magma composition with about 80% crystallization of a parent magma at two different oxygen fugacities using the model of Nielsen [1990]. The model predicts that olivine crystallizes first, followed by pyroxene, followed by magnetite, a sequence in agreement with the bulk rock chemistry and the petrography of the samples. Higher oxygen fugacities result in earlier crystallization of magnetite (heavy line). (b) MgO-K<sub>2</sub>O. Liquid lines of descent for two starting compositions with different K<sub>2</sub>O abundance (Table 2) are shown. Symbols are the same as in Figure 3.



**Figure 5.** Chondrite-normalized rare earth element patterns of Tahitian volcanics. Normalization values are slightly modified from the average of 20 ordinary chondrites reported by Nakamura [1974].

mantle source, as Pb/Ce ratios in Society Islands lavas correlate with isotope ratios (W. M. White, manuscript in preparation, 1994). Third, the central lavas have somewhat lower abundances of Ta and Nb. This feature is also associated with the source, as Nb/U ratios in Society Islands lavas correlate with isotope ratios (W. M. White, manuscript in preparation, 1994). Fourth, Zr and Hf of all groups are overabundant compared to rare earths of similar compatibility (e.g., Sm). Since Hf/Sm ratios in Society Islands lavas also correlate with isotope ratios, we believe this feature is real and associated with the Societies mantle plume. Finally, all lavas

have a negative K anomaly. The central lavas at first appear to be an exception; however, we believe these lavas also are K depleted, but this is disguised by low abundances of Ta and Nb. In addition, only the central lavas are depleted in Rb relative to Ba.

Three observations suggest that the K depletion is not related to weathering. First, the oldest (central) least depleted lavas (Figure 6) should have the greatest K depletion based on their degree of weathering. Second, weathering should produce greater depletions in Rb than K, but there are actually slight enrichments of Rb in the shield, late-stage, and Tahiti Iti

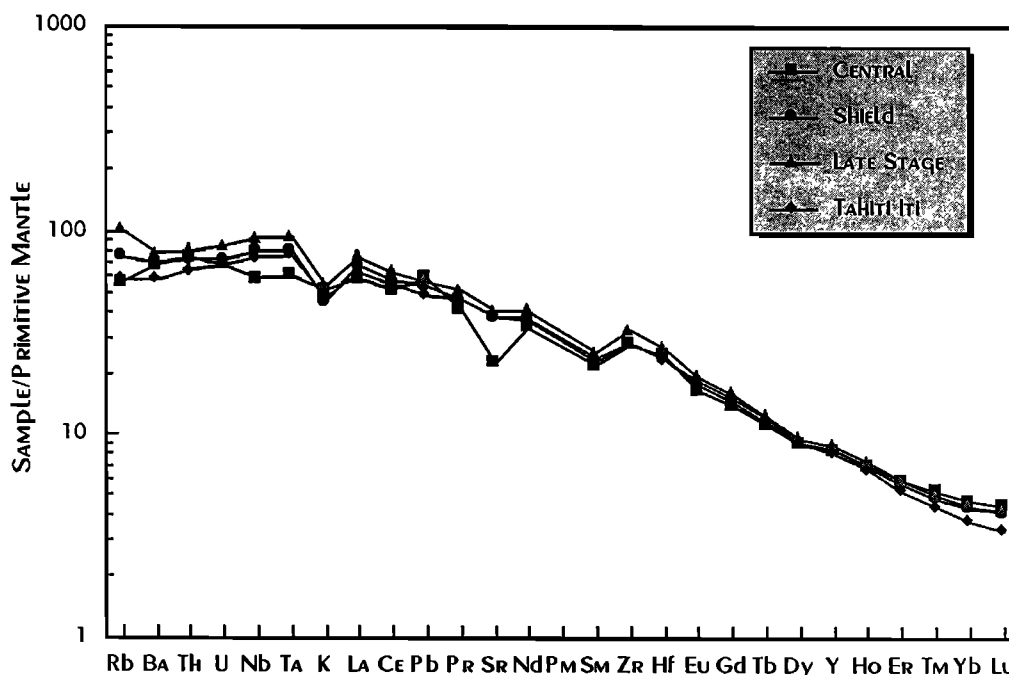


**Figure 6.** "Spider" diagram showing average abundances of incompatible elements in central, shield, late-stage, and Tahiti Iti lavas, normalized to a primitive mantle composition. Normalization values are from Sun and McDonough [1989].

lavas. Third, depletion of K by 30% (suggested by comparing K abundance with Ta and La abundance, Figure 6) would result in the calculated ages of the Punaruu Valley basalts being 30% too old and inconsistent with the well-dated paleomagnetic boundaries (Figure 2). The close agreement of the ICPMS potassium analyses with the atomic absorption spectrophotometric analyses (Table A1) shows no analytical bias. Hence we conclude that the K depletion of the Tahiti lavas must be a primary feature of these rocks. The only observed effect of weathering is the slight depletion of Rb in the central lavas.

In Figure 7,  $\epsilon_{Nd}$  is plotted against  $^{87}Sr/^{86}Sr$ . The Tahiti data fall entirely within the field defined by previously published Society Islands and Seamounts data [White and Hofmann, 1982; Devey et al., 1990]. Figure 8 displays Pb isotope ratios plotted in the usual manner. Again, our data fall with the field previously defined for the Societies. In contrast to the range of Sr and Nd isotope ratios, the range in Pb isotope ratios is notably restricted, a feature characteristic of the Societies in general [White, 1985; Devey et al., 1990]. The  $^{207}Pb/^{204}Pb$  and  $^{208}Pb/^{204}Pb$  isotope ratios reported by Cheng et al. [1993] are generally higher than our values, as discussed earlier. Sr and Nd isotope ratios are strongly correlated, a feature suggestive of two-component mixing. However, the correlations between Pb and Sr isotope ratios (Figure 9) and Pb and Nd isotope ratios (not shown) are very much poorer and would preclude the possibility that the source of Tahitian magmas, and Society magmas generally, is a mixture of two homogeneous components.

Cheng et al. [1993] found that Sr and Nd isotope ratios in Tahitian magmas decreased and increased, respectively, with time. Cheng et al. [1993] also argued that the three volcanic stages identified by Duncan et al. [1987] began with high Sr and low Nd isotope ratios that respectively decreased and increased with time. Our Nd isotope and age data, combined

with that of Cheng et al. [1993], are shown in Figure 10. The combined data clearly show a general decrease in  $^{87}Sr/^{86}Sr$  with time but do not support the idea that volcanic stages beginning at ~1.7 Ma, 1.25 Ma, and 0.8 Ma had initially high  $^{87}Sr/^{86}Sr$  that subsequently decreased. The temporal evolution of magma geochemistry in Tahiti appears to be broadly similar to that observed in Hawaii [e.g., Chen and Frey, 1985; Lanphere and Frey, 1987; Hofmann et al., 1987]. In both Hawaii and Tahiti, radiogenic isotope ratios shift toward more depleted signatures with time, and the magmas become increasingly silica undersaturated.

## Discussion

### Punaruu Sequence

This sequence is our best sampled eruptive series on the island and provides an opportunity to model the evolution of the magmatic system that produced these lavas. Much of the sequence was erupted over a period of 300,000 years. The chemical stratigraphy is shown in Figure 11;  $K_2O$  is used for this time series for a number of reasons. (1) It is a major element (> 1 wt. % in most samples), so it has been analyzed in all samples (only a subset of the rocks was analyzed for trace elements), and there does not appear to be any interlaboratory bias or significant differences between the various analytical methods. (2)  $K_2O$  is an incompatible element in the primary fractionating minerals, olivine, augite, and magnetite, so its abundance in the host magmatic liquid can be estimated from the bulk rock  $K_2O$  and the phenocryst abundances. (3) Pressures in crustal magma chambers have little effect on the partition coefficient of  $K_2O$  in the primary phenocrysts, so pressure has little effect on the  $K_2O$  in the magmas. This is important because even though our

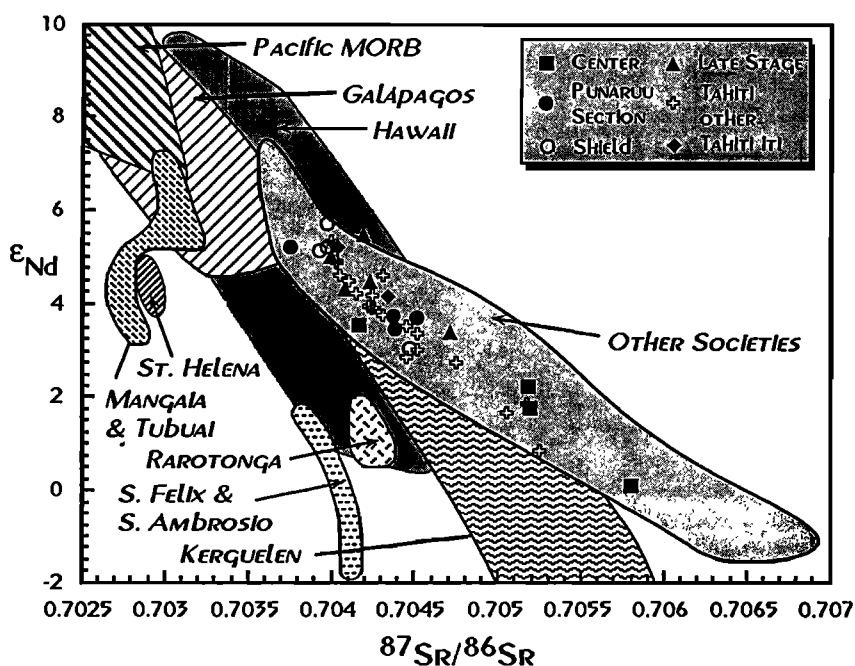


**Figure 7.** Sr and Nd isotopic ratios of volcanic rocks from Tahiti. The group "Tahiti other" includes the Smithsonian samples (Table A4), whose ages and stratigraphic positions are unknown, as well as data from Cheng et al. [1993]. Fields for literature data for mid-ocean ridge basalts (MORB), Galapagos, Kerguelen, Saint Helena, Tubuai and Mangaia, Rarotonga, San Felix, and San Ambrosio, and other Society Islands and seamounts are shown for comparison. Note the large range of the Tahitian data and the general linearity of the Societies array.



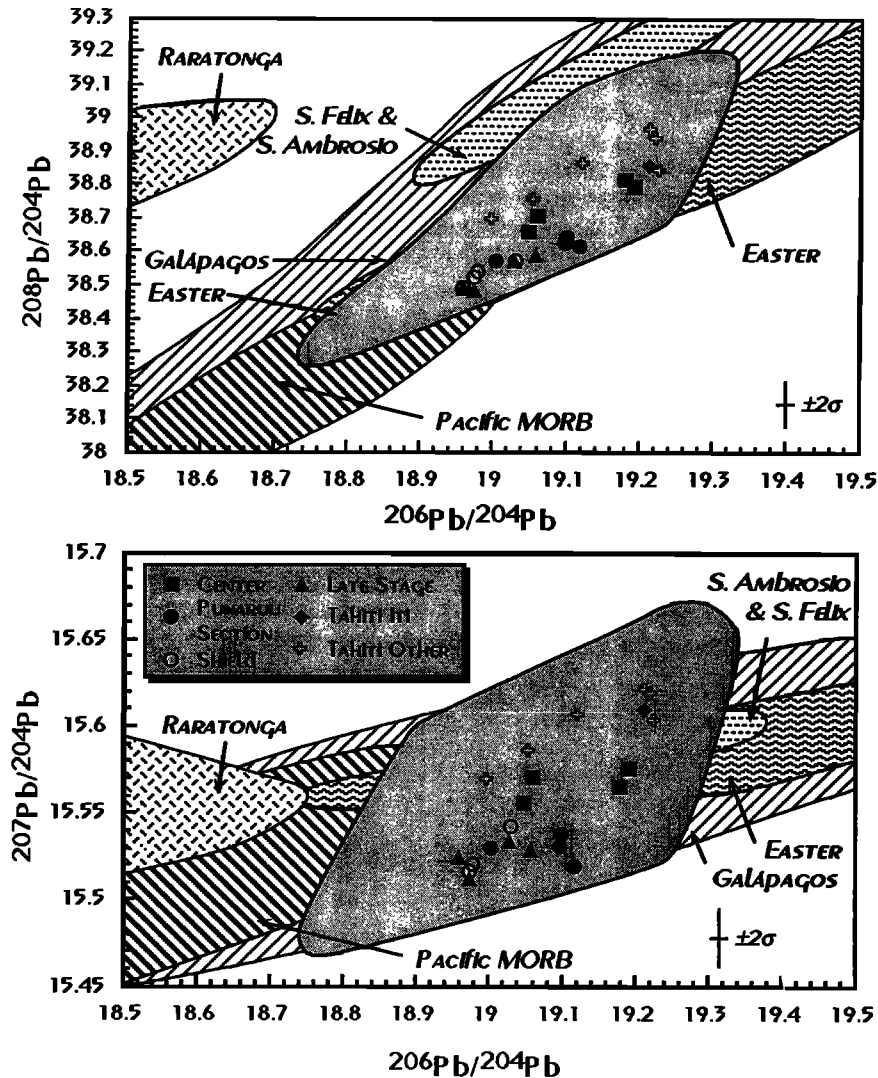


**Figure 8.** Pb isotope ratios in Tahitian lavas. Fields for literature data for mid-ocean ridge basalts (MORB), Galapagos, Easter, Tubuai and Mangaia, Raratonga, San Felix, and San Ambrosio, and other Society Islands and seamounts are shown for comparison. Note that the range of these plots is rather limited, reflecting the limited range in Pb isotope ratios in Societies lavas. For example, the field for Pb isotope ratios in Galapagos lavas extends off both ends of the plot.  $2\sigma$  error bars are shown for reference.

fractionation model was calibrated with data from 1-atm experiments, the models will be applicable to fractionation in a crustal magma chamber.

Our assumption that  $\text{K}_2\text{O}$  has behaved as an incompatible element (and appropriate to monitor magma evolution) is justified in a plot of  $\text{P}_2\text{O}_5/\text{K}_2\text{O}$  versus  $\text{K}_2\text{O}$  (Figure 12).  $\text{P}_2\text{O}_5/\text{K}_2\text{O}$  is uniform (at  $\sim 0.35$ ) over a wide range of  $\text{K}_2\text{O}$ ; hence  $\text{P}_2\text{O}_5$  and  $\text{K}_2\text{O}$  are equally incompatible within the range of fractionation, especially within the Punaruu section. We note, again, that there is no evidence for K loss from weathering, even in the central flows. A few late-stage lavas have higher  $\text{P}_2\text{O}_5/\text{K}_2\text{O}$ , due to higher  $\text{P}_2\text{O}_5$ .  $\text{K}_2\text{O}$  is also highly correlated with other incompatible elements (e.g., Zr) for the Punaruu flows, reiterating the consistently incompatible behavior of K during fractional crystallization.

The computer model used to evaluate the evolution of the Tahiti magmatic system is a modified version of the differentiation model of Nielsen [1990]. This model calculates the composition of magmatic liquids resulting from low-pressure fractional crystallization, magma chamber recharge,

and eruption. The modified model relies on experimental phase equilibrium and phase compositions of alkali basalts and on the observed phase equilibria of the Tahiti samples. Sample outputs of this calculation (for simple fractional crystallization) are shown in Figures 3 and 4.

The model requires that a number of initial conditions be specified: the composition of the parent magma, the oxygen fugacity within the magma chamber, and the processes operating within the magma chamber. The processes include: (1) homogeneous fractional crystallization with no recharge or eruption, which is depicted in Figures 3 and 4; (2) magma chamber recharge; and (3) eruption from the magma chamber. If processes (2) and (3) are permitted, then assumptions about their timing and the relative proportions of crystallization and eruption relative to recharge are required. In the models discussed here, recharge is assumed to occur after an amount of crystallization (for example, 10, 20, or 30%) within the magma chamber. However, the amount of crystallization between recharge events is allowed to vary in a Gaussian distribution about these specified values. The total of

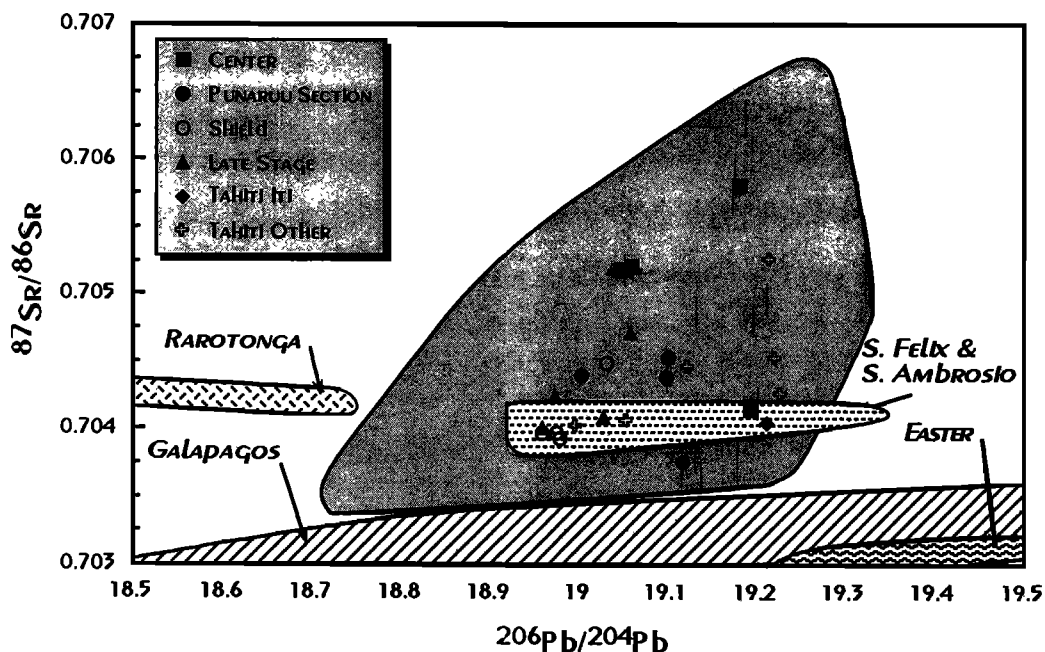


**Figure 9.** Relationship between Sr and Pb isotope ratios in Tahitian lavas. Fields for literature data for Galapagos, Easter, Tubuai and Mangaia, Rarotonga, San Felix and San Ambrosio, and other Society Islands and seamounts are shown for comparison. The correlation between  $^{87}\text{Sr}/^{86}\text{Sr}$  and  $^{206}\text{Pb}/^{204}\text{Pb}$  is poor, particularly in comparison to that between  $^{87}\text{Sr}/^{86}\text{Sr}$  and  $\epsilon_{\text{Nd}}$ .

crystallization plus eruption relative to recharge determines whether the magma chamber is growing, dying, or at steady state. We have examined dying magma chambers (no recharge, Figures 3 and 4) and steady state magma chambers (recharge equals crystallization plus eruption, Figure 11).

The parental magma was estimated with a method previously used for a suite of ocean island basalts [Fisk *et al.*, 1988]. The

range of FeO (total) abundance in rocks with high MgO is relatively restricted, especially for the shield lavas (Figure 4a), and this trend is due to the accumulation or crystallization of olivine. The most primitive olivines found in this suite of lavas are  $\text{Fo}_{39}$ . This constraint, along with the limited range of FeO (11 to 12 wt. %) and the established iron-magnesium  $K_D$  for olivine-basalt equilibrium [Roeder and Emslie, 1970],

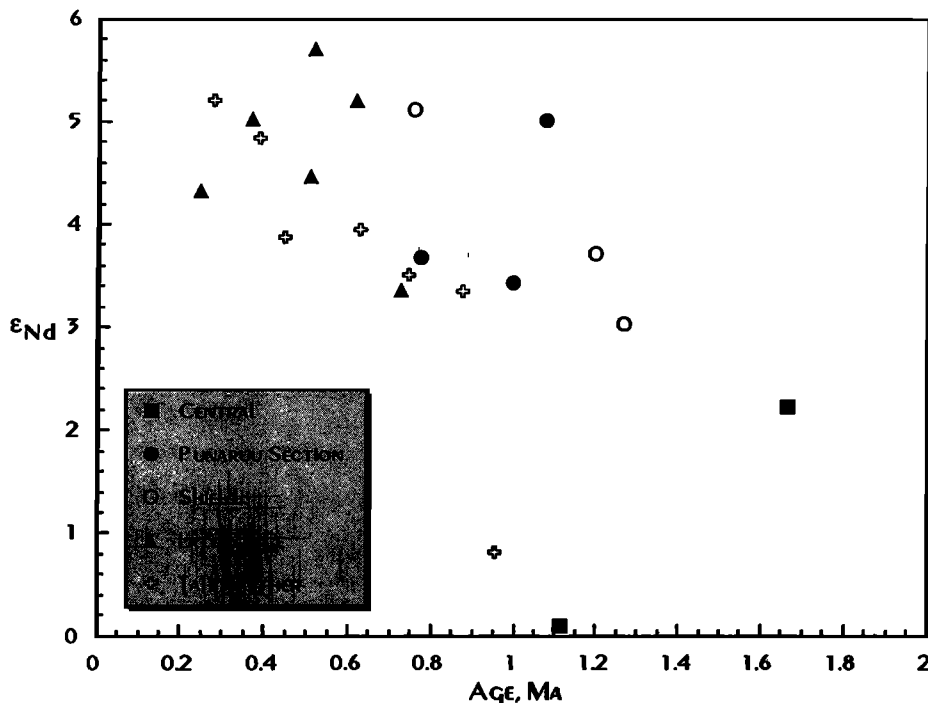


**Figure 10.**  $\epsilon_{\text{Nd}}$  plotted against age for Tahitian lavas. "Other" includes data from Cheng *et al.* [1993]. There is a systematic change to more depleted, or more MORB-like, isotopic compositions with time, although the two lavas with the least radiogenic compositions erupted between 1.2 and 1.0 Ma.

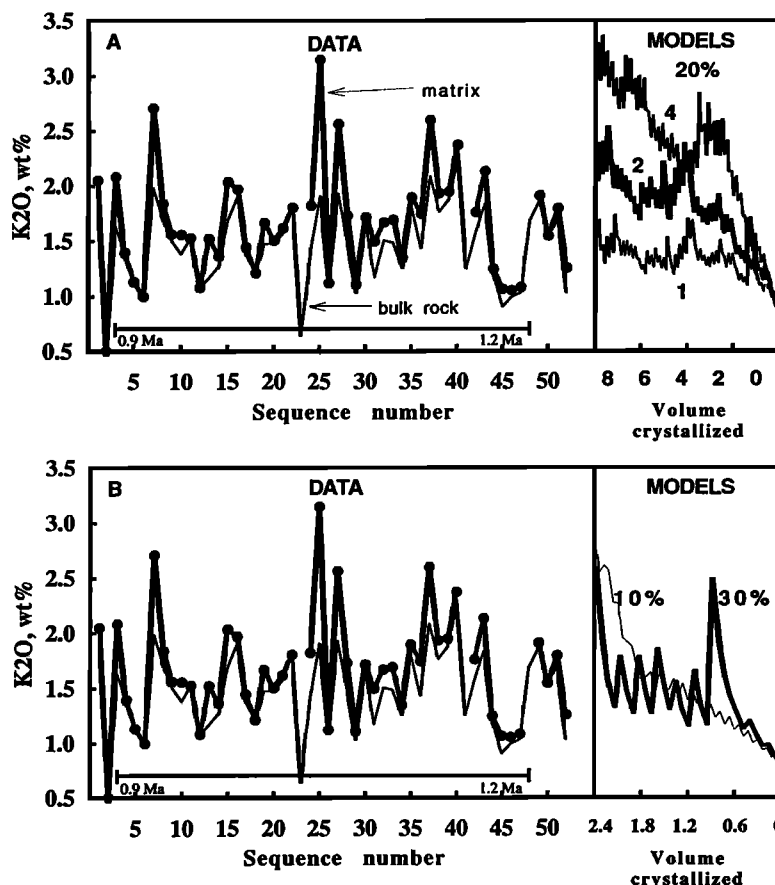


**Figure 11.**  $K_2O$  variation with position in the Punaruu Valley section and computer-generated magma compositions. The sequence numbers correspond to those in electronic supplement Table A1. In the left hand panels the light line is the whole rock abundance, and the heavy line with solid circles has been corrected for phenocryst content. The line at the bottom shows the 0.3 m.y. interval over which most lavas were erupted. Lavas 3 to 23 were erupted in a period of about 50,000 years. (a) The right panel shows the effect of changing the ratio of crystallization to eruption ( $C/E$ ) in a steady state magma chamber. As  $C/E$  increases, the steady state  $K_2O$  abundance increases. In all models the amount of crystallization between recharge events averages 20%. Volume crystallized indicates the amount of crystallization relative to the original magma chamber volume. (b) The right panel shows the effect of changing the average amount of crystallization between recharge events in the case where  $C/E = 2$ .

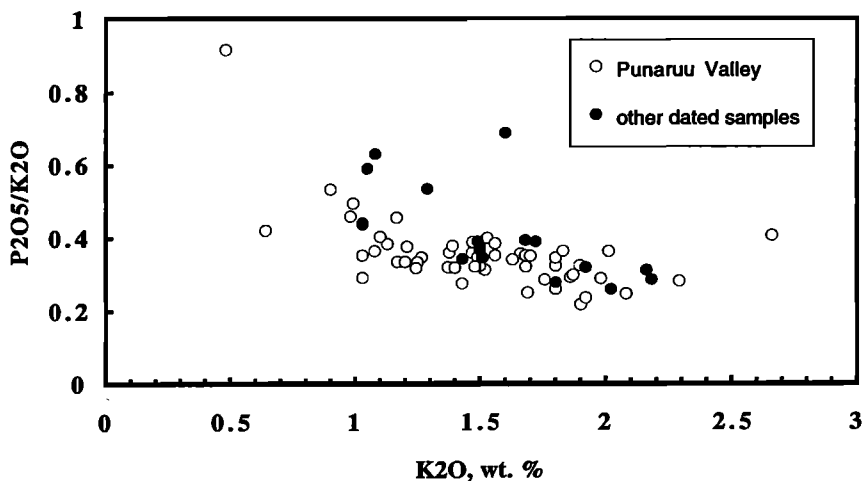


**Figure 12.** For the majority of the Punaruu basalts and other dated samples,  $P_2O_5/K_2O$  is uniform (at  $\sim 0.35$ ), indicating that  $K_2O$  and  $P_2O_5$  are equally incompatible and that K loss during weathering has not been a significant concern. A few samples, all from late-stage lavas, have high  $P_2O_5/K_2O$  due to higher  $P_2O_5$  contents.

requires an MgO content of the parent magma of 13 to 14.2 wt. %. Other oxide abundances within this parent magma can be estimated (Table 2) by examining MgO-oxide variation diagrams (such as Figure 4b).

The chemical differences between the main shield-building phase of volcanism and the late-stage volcanism suggest that there was a change in composition of the parent magmas for the two series. These differences are obvious in Figures 3 and 4 with the late-stage basanites having lower SiO<sub>2</sub> and higher FeO and K<sub>2</sub>O than do the shield-building alkali basalts. The estimated parent magmas for the shield and late-stage basalts are given in Table 2.

The oxygen fugacity of the magma chamber is also important for these models because it controls the appearance of magnetite, which when fractionated strongly affects the SiO<sub>2</sub>, TiO<sub>2</sub>, and FeO abundance of the lavas (Figures 3 and 4). In Figure 3 the liquid line of descent is shown for magmas buffered at two oxygen activities. In the more oxidized magma, magnetite starts to crystallize shortly after pyroxene, resulting in a nearly continuous increase in silica with increasing differentiation. In the less oxidized magma, magnetite formation is delayed so the crystallization sequence of olivine, olivine plus pyroxene, and olivine plus pyroxene plus magnetite results in a zigzag path of silica abundance (Figure 3). These models indicate that the oxygen fugacity decreased as the shield-building volcanism gave way to late-stage volcanism. This supports our hypothesis (developed below) that the mantle source of the Tahitian magmas evolved from OIB or plume (more oxidized [Ballhaus, 1993]) to a MORB or upper mantle source (less oxidized).

The computer model calculates the composition of the residual liquid for every 0.2% crystallization. These calculated compositions should be compared with the liquids erupted from the magma chamber. The compositions of the lavas that we report, however, include phenocrysts, so we cannot make a direct comparison of the calculated liquids from the models with these bulk rock compositions. We have therefore determined the modal abundance of phenocrysts (by point counting) for most of the Punaruu Valley basalts and corrected the bulk rock chemistry accordingly. The effect of this correction on K<sub>2</sub>O can be seen in Figure 11. The most evolved magmas (with the highest K<sub>2</sub>O) also tend to have the highest phenocryst abundance so that the variation in matrix K<sub>2</sub>O (heavy line, Figure 11) has the same pattern as that for the bulk rock K<sub>2</sub>O (light line, Figure 11) but a larger amplitude.

The majority of the Punaruu Valley lava flows that we examined (46 samples in about 700 m of section) erupted over 300,000 years. They may be considered a random sample of the magmatic system at approximately 6500-year intervals. Our models have assumed a single magma chamber erupting and recharging over this period, but we cannot dismiss the possibility of several independent chambers operating contemporaneously or in sequence. However, we see no long-term trends in composition of the majority of Punaruu lavas, although there is a significant increase in P<sub>2</sub>O<sub>5</sub> in the youngest lavas, consistent with the shift to more alkalic lavas at about 0.9 Ma.

The presence of 23 lavas within the Jaramillo reversed period (about 50,000 years) suggests that these eruptions occurred, on average, every 2000 years. Within this 50-kyr period there are three series of four or more lavas, characterized by a progressive increase in K<sub>2</sub>O followed by a sudden decrease in K<sub>2</sub>O. These series may represent episodes of magma chamber shrinkage followed by recharge, with mean duration of 15,000 to 20,000 years. *Leotot et al.* [1990] documented a similarly detailed history of eruptive cycles in the construction of the western portion of Tahiti Iti, each lasting approximately 13,000 years.

We have modeled steady state magma chamber processes (Figure 11) and found that the ratio of crystallization to eruption (C/E) determines the average level of differentiation of the steady state lavas. This point is illustrated (Figure 11a, right panel) with the continuous composition of the magma chamber for three C/E values. The lowest curve (labeled 1) is for equal amounts of crystallization and eruption (C/E = 1), and the middle and upper curves are for C/E values of 2 and 4, respectively. The curves all start at the K<sub>2</sub>O content of the parent magma and approach steady state K<sub>2</sub>O abundances of about 1.3 wt. %, 2.2 wt. %, and 3.2 wt. % with increasing C/E value.

Another feature of the steady state models is that high C/E corresponds to a slow approach to the steady state abundance of K<sub>2</sub>O. The full scale in the right panel of Figure 11a represents 800% crystallization of the magma chamber (eight magma chamber volumes), and K<sub>2</sub>O abundance reaches a steady state value of about 3.2 wt. % when C/E = 4 only after about 800% crystallization. For a C/E = 1 the steady state value is approached after about 200% crystallization. Since crystallization plus eruption equals recharge (C + E = recharge), the models 1, 2, and 4 (Figure 11a) reach a steady state after recharge volumes that are 4, 6, and 10 times the volume of the magma chamber. The best fit average K<sub>2</sub>O abundance in the Punaruu section (after correction for phenocryst content) appears to be for models where C/E = 1 to 2 (Figure 11a), in which 50 to 67% of the recharged magma crystallizes in the magma chamber and the remainder erupts. These models match the average K<sub>2</sub>O abundance, but the amplitude of the K<sub>2</sub>O variations in the steady state magma chamber (Figure 11a, right panel) is much smaller than the observed variations of K<sub>2</sub>O (Figure 11a, left panel).

In the three models of Figure 11a, the average amount of crystallization between recharge events was 20%, which results in an average amplitude of variation of K<sub>2</sub>O between recharge events of 0.2 to 0.4 wt. %. The amount of crystallization between recharge events varied randomly about this 20% value, simulating an unsteady recharge of the magma chamber and irregular variation in magma chamber chemistry. Figure 11b shows the results of the crystallization model in which the C/E = 2 and the average amount of crystallization between recharge events was either 10% or 30%. The amplitude of the variations of the magma chamber chemistry for the 30% model is similar to that for the variations observed in Punaruu Valley flows but the amplitude of the K<sub>2</sub>O variations for the 10% model is much smaller than observed.

**Table 2.** Starting Compositions for Models

Suite	SiO <sub>2</sub>	Al <sub>2</sub> O <sub>3</sub>	FeO	Fe <sub>2</sub> O <sub>3</sub>	MgO	CaO	Na <sub>2</sub> O	K <sub>2</sub> O	TiO <sub>2</sub>	P <sub>2</sub> O <sub>5</sub>	Mn
Shield	46.4	10.5	10.0	2.0	13.8	10.9	2.0	0.8	2.8	0.40	0.20
Late stage	44.0	10.8	10.7	1.9	13.8	11.2	2.5	1.0	3.3	0.55	0.20

Values are given in weight percent.

For the 10% model to apply to the Punaruu section, successive magmas must have sampled the chamber at intervals separated by large amounts of crystallization. The 23 lavas within the Jaramillo reversed period suggest that these magmas erupted in rapid sequence and therefore do not represent eruptions separated in time by large amounts of crystallization and magma chamber recharge. They are therefore probably derived from a magma chamber that expressed a wide range of crystallization over a short period of time, as is illustrated by the model with 30% crystallization between recharge events.

### The Temporal Evolution of Tahitian Volcanism

An important feature of Tahitian rock compositions is the systematic variation in time that is apparent in isotope ratios and major element chemistry. As lava chemistry became increasingly silica undersaturated, the Sr and Nd isotope ratios shifted toward more depleted, more MORB-like, signatures. In light of this, the lack of systematic variation in incompatible element abundances or ratios is remarkable. The changes in  $^{87}\text{Sr}/^{86}\text{Sr}$  and  $\epsilon_{\text{Nd}}$  imply that the mantle source became more depleted in incompatible elements with time, which should be reflected in the incompatible element abundances of the lavas if all other factors remain constant. The only reasonable inference that can be drawn from the constancy of incompatible element ratios such as La/Sm is that the degree of melting must have decreased through time.

To illustrate this point, we have superimposed some simple model calculations on a plot of  $\epsilon_{\text{Nd}}$  versus  $[\text{La}/\text{Sm}]_{\text{N}}$  in Figure 13. We assumed that the source of Tahitian magmas is a

simple two-component mixture of depleted upper mantle (i.e., MORB source) and the Society mantle plume. (We noted earlier that the Pb isotope data preclude such a simple two-component model of the source. We nevertheless feel that comparison of the data with such a model is useful, and we return to the implications of the Pb isotope data at the end of this section.) For the depleted upper mantle, we assumed an  $\epsilon_{\text{Nd}}$  of 9.8 and a  $[\text{La}/\text{Sm}]_{\text{N}}$  of 0.4, which would give rise to a typical light rare earth depleted MORB upon 15% melting. For the plume (the enriched end-member), we assumed an  $\epsilon_{\text{Nd}}$  of -1, which is equal to the lowest  $\epsilon_{\text{Nd}}$  observed in the Society Islands (sample 73-185 from Tahaa [White and Hofmann, 1982]). We then calculated the rare earth abundances for the source of 73-185 using simple batch melting. (More complex melting models do not give substantially different results.) In doing so, we assumed 15% melting of garnet peridotite, based on the reasoning that the plume should be at least as hot as surrounding upper mantle and therefore that degree of melting should be at least as great as is typical of MORB, and we somewhat arbitrarily assumed 33% olivine fractionation. The  $[\text{La}/\text{Sm}]_{\text{N}}$  calculated for the plume from these assumptions was 3.08. From the  $\epsilon_{\text{Nd}}$  and rare earth abundances of the two model end-members, we calculated the mixing line shown by the heavy line in Figure 13. Dashed lines in Figure 13 show the calculated composition of 10%, 5%, 2%, and 1% partial melts of this mixture. Implicit in this model is the assumption that the mineralogy of the plume does not differ substantially from that of the asthenosphere.

The mixing line shows that La/Sm and  $\epsilon_{\text{Nd}}$  in the source should be inversely related. No such inverse relationship is

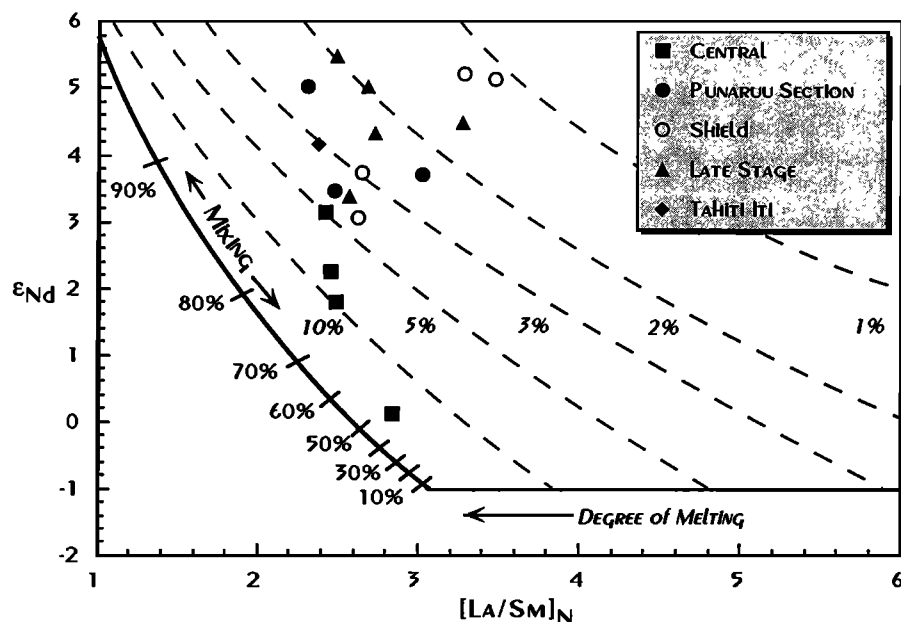


**Figure 13.**  $\epsilon_{\text{Nd}}$  plotted versus chondrite-normalized La/Sm ratio for Tahitian basalts (data from differentiated rocks are not plotted). Superimposed on the data is a mixing melting model. The heavy line represents mixing between the assumed composition of the Society plume ( $\epsilon_{\text{Nd}} = -1$ ,  $[\text{La}/\text{Sm}]_{\text{N}} = 3.08$ , La = 0.2 ppm, Nd = 0.84 ppm, and Sm = 0.32 ppm) and depleted mantle ( $\epsilon_{\text{Nd}} = +9.8$ ,  $[\text{La}/\text{Sm}]_{\text{N}} = 0.4$ , La = 8.1 ppm, Nd = 9.3 ppm, and Sm = 1.6 ppm). Labeled ticks show the percentage of depleted mantle in the mixture. Dashed lines labeled in italics show the composition of 1, 2, 3, 5, and 10% melts of this mixture. These calculations assume melting occurs in the garnet stability field, but the results would not be greatly different for melting of spinel peridotite. Comparison of the actual data with this model shows that the percentage of melting must decline as the fraction of depleted mantle in the source increases.

apparent in the actual data. Indeed, the most light rare earth enriched melts are associated with the highest  $\epsilon_{Nd}$ . Comparison of the data with our calculated mixing-melting model clearly indicates that the magmas with highest  $\epsilon_{Nd}$  must have been produced by the smallest degree of melting. Since  $\epsilon_{Nd}$  increases with time in Tahitian magmas, this suggests that the degree of melting decreased with time. Assuming that our estimates about the degree of melting for MORB and 73-185 are correct (i.e., both are 15% melts), then the earliest central magmas were produced by 5-15% melting while the late shield and late-stage magmas were produced by as little as 1-2% melting. Even if our estimate of the specific amount of source melting is incorrect, the degree of melting apparently declined by an order of magnitude over the course of Tahitian volcanism. Our conclusions in this respect are entirely consistent with those of *Cheng et al.* [1993].

If the most radiogenic Tahaa sample (73-185) represents the isotopic composition of the Societies mantle plume, then even the most enriched Tahitian samples are derived from a mixed source that contains nearly 40% depleted mantle. In the simple two-component model illustrated in Figure 13, the late-stage samples with highest  $\epsilon_{Nd}$  are derived from a source consisting predominantly of depleted mantle with less than 10% admixture of the Societies plume.

The progression to a more depleted source and to small degrees of melting in Tahiti is similar to that observed in Hawaii. *Chen and Frey* [1985] proposed that the compositional evolution of Hawaiian volcanoes reflects passage of the volcano over the plume. We adopt a similar model to explain our observations on Tahiti (Figure 14). Our model differs from theirs in that we argue that the depleted signature of the late-stage magmas primarily reflects melting of depleted mantle entrained by the plume rather than melting of the lithosphere.

In our model, volcanic evolution at Tahiti reflects the rheological and thermal interaction between the plume and the surrounding mantle. Mantle viscosities are in the range of  $10^{18}$  to  $10^{22}$  P. Plumes appear to be typically 200°C or more hotter than normal upper mantle [e.g., *Klein and Langmuir*, 1987; *Sleep*, 1990]. The assumed temperature dependence of viscosity of

$$\eta = \eta_0 \exp(-\beta\Delta T/T')$$

with  $\beta = 35$ ,  $T' \approx 2300^\circ\text{K}$  and  $\Delta T \approx 200^\circ\text{K}$  [*Stacey and Loper*, 1983; *Richards et al.*, 1988] implies a plume viscosity only 1 to 2 orders of magnitude lower than surrounding mantle. These viscosities mean that a vertical, axisymmetric plume cannot rise freely through the mantle; instead, surrounding mantle will be viscously coupled to the plume and rise with it as a sheath-like boundary layer. The thickness of this entrained layer could reach hundreds of kilometers [*Hauri et al.*, 1993]. Conductive heat loss from the plume to the boundary layer causes further reduction in viscosity contrast and increases the buoyancy of the boundary layer material [*Griffiths*, 1986]. Thus the plume will continuously entrain surrounding mantle as it rises, so that material closest to the plume core will have been entrained from the deepest levels, while the outer part is entrained at relatively shallow levels (Figure 14). This produces, in plan view, a concentrically zoned hotspot, with the most plume-like material in the center, followed by lower and upper mantle material with increasing radius. The entire

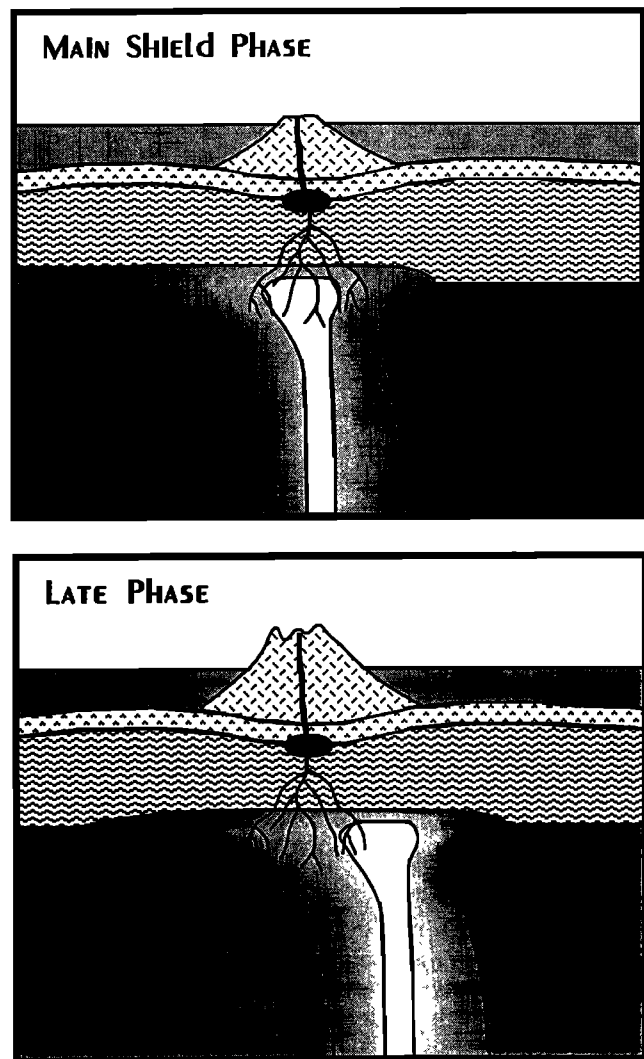


**Figure 14.** Cartoon illustrating how volcanic evolution of Tahiti is controlled by passage over a chemically and thermally zoned plume. Shading is used to suggest variations in temperature and consequently extent of melting. The central core of the plume, consisting of deep mantle incompatible element enriched and radiogenic material, is hottest. Temperatures in the surrounding incompatible element depleted and less radiogenic material, entrained through viscous coupling and heating by the rising plume, decrease radially away from the central core. In the main shield phase, magmas contain a relatively large fraction of high-degree melts derived from the plume core. In the late stage, the contribution from the core is small, and the bulk of the magmas is derived by smaller extents of melting of the cooler margins.

rising structure will pass through the P,T conditions for melting in the upper mantle; however, temperatures in the peripheral material will remain substantially below that of the plume core, so that the entrained mantle will melt to a lesser degree than the initial plume mantle. This melting range is reinforced by the fact that upper mantle, being more depleted in incompatible elements, will melt less at a given temperature than will plume mantle. We assume that the volcano is located directly over the plume core during its most vigorous period of growth in the early shield stage (central lavas). As the volcano is transported away from the plume by plate motion, small-

degree melts of the cooler sheath increasingly dominate the waning volcanic activity.

Cheng *et al.* [1993] suggested that the depleted component in Tahitian lavas was derived from metasomatized lithosphere. While melting of the lithosphere may contribute in a minor way to Tahitian volcanism, we believe, primarily on the basis of thermal considerations, that it is a less satisfactory source for the depleted component than is entrained depleted mantle. The 60 Ma lithosphere, particularly in its mid and upper regions, would have cooled well below its melting temperature. Cheng *et al.* [1993] proposed conductive heating by the plume. However, conduction is a particularly slow means of transmitting heat in the mantle. Emerman and Turcotte [1983] concluded that conductive heating of the lithosphere by a plume is not likely to be significant.

In addition, the mid and upper portion of the lithosphere would have been severely depleted in its basaltic component and incompatible elements by melting at a spreading center and hence would be a poor source of basalt. Partly on the basis of their analysis of Tahitian xenoliths, Cheng *et al.* [1993] dismissed this problem by suggesting that the lithosphere beneath Tahiti had been "metasomatized." Cheng *et al.* [1993, p. 177] suggested no specific mechanism for this metasomatism but stated only that it "may be related to the 'superswell' proposed by McNutt and Fischer [1987]." On the basis of the similarity between the isotopic compositions of Tahitian xenoliths analyzed by Cheng *et al.* ( $\epsilon_{\text{Nd}} \sim +4$  and  $^{87}\text{Sr}/^{86}\text{Sr} \sim 0.7042$ ) and Tahitian magmas, we suggest that the "residual" xenoliths acquired their isotopic compositions by reaction with Tahitian plume magmas that had earlier passed through the lithosphere, i.e., the agent of metasomatism was simply earlier Tahitian magmas. We see no compelling evidence in our data for the existence of "metasomatized" lithosphere prior to Tahitian magmatism.

One important contrast with Hawaiian volcanism is that while tholeiites predominate in Hawaii, alkali basalts predominate in the Societies. The data we report here, as well as those of Cheng *et al.* [1993] and LeRoy *et al.* [1993], demonstrate that hypersthene-normative lavas do exist in the earliest exposed sequences. However, even if tholeiites predominate at some deeper, unexposed level, the tholeiite-alkali basalt transition would appear to occur at a much earlier point in the evolution of Tahiti than is typical of Hawaiian volcanos.

There are two factors that may explain this predominance of alkali basalts. First, because they reflect higher time-integrated Rb/Sr and Nd/Sm, the isotopic data require that the Society plume source has been more enriched in incompatible elements, including K and Na, than the Hawaiian plume source. Thus even at similar concentrations of SiO<sub>2</sub>, Tahitian magma compositions will be more alkalic than Hawaiian magmas. Second, the Society plume has a significantly lower buoyancy flux than does the Hawaiian plume [Sleep, 1990]. This may indicate that the Society plume is cooler than the Hawaiian one. If so, the degree of melting will generally be lower. Magmas produced by lower degrees of melting are typically poorer in SiO<sub>2</sub> and richer in alkalis and hence will be more alkalic than higher-degree melts.

We now return to the lack of correlation between Pb isotope ratios and Sr and Nd isotope ratios. This observation would seem to rule out the simple two-component mixing model proposed here. However, we emphasize that the total range in Pb isotope ratios in Tahiti is small compared to that of other

oceanic islands such as the Galapagos. Heterogeneity in Pb isotope ratios in either end-member, despite uniformity in Sr and Nd isotope ratios, may explain the lack of correlation in Figure 8. Alternatively, the Pb isotope ratios may indicate the presence of a third component. One possible component is FOZO ("focal zone"), the composition that Hart *et al.* [1992] hypothesize to characterize the lower mantle. The Sr and Nd isotope compositions of FOZO lie close to the "enriched" end of the MORB array. Because of this, a three-component mixture of depleted mantle, FOZO, and the Society plume may still produce a relatively linear array on a plot of Nd versus Sr isotope ratios. The Pb isotope composition of FOZO is more radiogenic than that of MORB, so a plot of Sr versus Pb isotope ratios would show the weak correlation characteristic of three-component mixtures. In the context of the model we propose, the FOZO material would have been entrained from the lower mantle, while depleted mantle would have been entrained at shallower levels. With the existing data, we cannot distinguish between these two possibilities or verify the presence of FOZO in the Tahitian source. Additional data, particularly He isotope data, might ultimately resolve this question.

### Nature of the Society Mantle Plume

White and Hofmann [1982] suggested that the distinctive isotopic compositions of the Society mantle plume reflect the presence of subducted oceanic crust and sediment in the plume. High Pb/Ce ratios in Society seamount lavas reported by Devey *et al.* [1990] provided some support for this hypothesis. Newsom *et al.* [1986] showed that Pb/Ce ratios in MORB and many oceanic island basalts have uniform values of about 0.036. This value is substantially below the bulk earth value of about 0.1 and lower than Pb/Ce ratios in the continental crust, which are generally in excess of 0.1. Ben Othman *et al.* [1989] found that modern marine sediments also have values in excess of 0.1 and noted that because of the relatively high concentrations of Pb in sediment and the low concentration of Pb in the mantle the Pb/Ce ratio should be a particularly sensitive indicator of the presence of recycled sediment in mantle plumes. White *et al.* [1993] have found that Pb/Ce ratios in Tahaa basalts range up to 0.064, which is well above the range found in other oceanic basalts by Newsom *et al.* [1986]. In Tahiti, most basalts have Pb/Ce ratios in the range of 0.033 to 0.042, typical of oceanic basalts generally. However, several of the central lavas have higher Pb/Ce ratios, ranging up to 0.050. Furthermore, Pb/Ce ratios in Societies basalts, including the Tahitian samples reported here, correlate strongly with Sr and Nd isotope ratios [White *et al.*, 1993]. This correlation demonstrates that the elevated Pb/Ce ratios are a feature of the source, and it strongly suggests the incompatible element enrichment that characterizes the plume is due, at least in part, to deep recycling of crustal material.

### Conclusions

The ages of the subaerial lavas at the island of Tahiti, which make up about 2% of the volume of the volcanic system, range from 1.7 to 0.2 Ma. The majority of these lavas appear to have erupted between 1.3 and 0.9 Ma. This episode was followed by a period of less voluminous posterosional eruptions. Through the construction of the volcano the lava

compositions changed from tholeiitic and alkalic basalts to basanites, while corresponding Sr and Nd isotopic ratios changed to more depleted values. We interpret these trends to indicate that the mantle source for melting changed from a predominantly plume composition to depleted upper mantle with time. We propose that a compositional zonation occurs across the Societies hotspot, as a result of entrainment of depleted mantle around the rising plume. During the vigorous shield-building phase of volcanism the magma chamber was recharged at intervals separated by about 30% crystallization of the magma chamber. More than three recharge events are observed during the 50,000 year Jaramillo (magnetic normal) period, suggesting that these events occurred roughly 20,000 years apart.

**Acknowledgments.** We thank Jacques Talandier (Atomic Energy Commission, Papeete) and ORSTOM for hospitality and logistical support in Tahiti, Hans Barszczus and Jim Natland for assistance in sampling and discussions, Pierrick Roperch and Annick Chauvin for paleomagnetic core samples from the Punaruu Valley, and Mike Cheatham and Karen Harpp for assistance with the isotopic analyses. The paper has been improved following reviews by Fred Frey, Eric Hauri, Pierre-Yves Gillot, and Don Swanson. R.A.D. and M.R.F. were supported by NSF grant EAR85-09012, and W.M.W. by NSF grant EAR87-07484.

## References

- Ballhaus, C., Redox states of lithospheric and asthenospheric upper mantle, *Contrib. Mineral. Petrol.*, **114**, 331-338, 1993.
- Becker, M., R. Brousse, G. Guille, and H. Bellon, Phases d'érosion - comblement de la vallée de la Papenoo et volcanisme subrecent a Tahiti, en relation avec l'évolution des îles de la Société (Pacifique Sud), *Mar. Geol.*, **16**, 71-77, 1974.
- Ben Othman, D., W. M. White, and J. Patchett, The geochemistry of marine sediments, island arc magma genesis, and crust-mantle recycling, *Earth Planet. Sci. Lett.*, **94**, 1-21, 1989.
- Binard, N., R. C. Maury, G. Guille, J. Talandier, P.Y. Gillot, and J. Cotten, Mehetia Island, South Pacific: Geology and petrology of the emerged part of the Society hot spot, *J. Volcanol. Geotherm. Res.*, **55**, 239-260, 1993.
- Chauvin, A., P. Roperch, and R. A. Duncan, Records of geomagnetic field reversals from volcanic islands of French Polynesia, 2, Paleomagnetic study of a flow sequence (1.2-0.6 Ma) from the island of Tahiti and discussion of reversal models, *J. Geophys. Res.*, **95**, 2727-2752, 1990.
- Cheatham, M. M., W. F. Sangrey, and W. M. White, Sources of error in external calibration ICP-MS analysis of geological samples and an improved non-linear drift correction, *Spectrochim. Acta B*, **48**, E487-E506, 1993.
- Cheminee, J. L., R. Hekinian, J. Talandier, F. Albarede, C. W. Devey, J. Francheteau, and Y. Lancelot, Geology of an active hot spot: Teahitia-Mehetia region in the south central Pacific, *Mar. Geophys. Res.*, **11**, 27-50, 1989.
- Chen, C.-Y., and F. A. Frey, Trace element and isotopic geochemistry of lavas from Haleakala Volcano, east Maui, Hawaii: Implications for the origin of Hawaiian basalts, *J. Geophys. Res.*, **90**, 8743-8768, 1985.
- Cheng, Q. C., J. D. Macdougall, and G. Lugmair, Geochemical studies of Tahiti, Teahitia and Mehetia, Society Island chain, *J. Volcanol. Geotherm. Res.*, **55**, 155-184, 1993.
- DeNeufbourg, G., Notice explicative sur la feuille Tahiti, scale 1/40,000, Bur. Rech. Geol. Min., Paris, 1965.
- Desonie, D. L., R. A. Duncan, and J. M. Natland, Temporal and geochemical variability of products of the Marquesas hotspot, *J. Geophys. Res.*, **98**, 17649-17665, 1993.
- Devey, C. W., F. Albarede, J. L. Cheminee, A. Michard, R. Muhe, and P. Stoffers, Active submarine volcanism on the Society hotspot swell (West Pacific): A geochemical study, *J. Geophys. Res.*, **95**, 5049-5067, 1990.
- Dostal, J., C. Dupuy, and J. M. Liotard, Geochemistry and origin of basaltic lavas from Society Islands, French Polynesia (south central Pacific Ocean), *Bull. Volcanol.*, **45**, 51-62, 1982.
- Duncan, R. A., Linear volcanism in French Polynesia, Ph.D. thesis, 151 pp., Aust. Natl. Univ., Canberra, 1975.
- Duncan, R. A. and D. A. Clague, Pacific plate motion recorded by linear volcanic chains, in *The Ocean Basins and Margins*, vol. 7A, edited by A. E. M. Nairn, F. G. Stehli, and S. Uyeda, pp. 89-121, Plenum, New York, 1985.
- Duncan, R. A., and I. McDougall, Linear volcanism in French Polynesia, *J. Volcanol. Geotherm. Res.*, **1**, 197-227, 1976.
- Duncan, R. A., M. T. McCulloch, H. G. Barszczus, and D. R. Nelson, Plume versus lithospheric sources for melts at Ua Pou, Marquesas Islands, *Nature*, **322**, 534-538, 1986.
- Duncan, R. A., M. R. Fisk, and J. Natland, The development of volcanism at Tahiti, French Polynesia, (abstract) *Eos Trans. AGU*, **68**, 1521, 1987.
- Dymond, J., K-Ar ages of Tahiti and Moorea, Society Islands, and implications for the hot-spot model, *Geology*, **3**, 236-240, 1975.
- Emerman, S. H., and D. L. Turcotte, Stagnation flow with a temperature-dependent viscosity, *J. Fluid Mech.*, **127**, 507-517, 1983.
- Fisk, M. R., B. G. J. Upton, C. E. Ford, and W. M. White, Geochemical and experimental study of the genesis of magmas of Reunion Island, Indian Ocean, *J. Geophys. Res.*, **93**, 4933-4950, 1988.
- Gillot, P.-Y., J. Talandier, H. Guillou, and I. LeRoy, Temporal evolution of the volcanism of Tahiti Island: Geology and structural evolution, paper presented at International Workshop on Intraplate Volcanism: The Polynesian Plume Province, August 2-7, Centre National de la Recherche Scientifique, Papeete, Tahiti, 1993.
- Griffiths, R. W., The differing effects of compositional and thermal buoyancies on the evolution of mantle diapirs, *Phys. Earth Planet. Inter.*, **43**, 261-273, 1986.
- Gurnis, M., and G. F. Davies, Mixing in numerical models of mantle convection incorporating plate kinematics, *J. Geophys. Res.*, **91**, 6375-6395, 1986.
- Hart, S. R., E. H. Hauri, L. A. Oschmann, and J. A. Whitehead, Mantle plumes and entrainment: Isotopic evidence, *Science*, **256**, 517-520, 1992.
- Hauri, E. M., J. A. Whitehead, and S. R. Hart, Fluid dynamic constraints on mixing in mantle plumes, paper presented at International Workshop on Intraplate Volcanism: The Polynesian Plume Province, August 2-7, Centre National de la Recherche Scientifique, Papeete, Tahiti, 1993.
- Hofmann, A. W., M. D. Feigenson, and I. Raczek, Kohala revisited, *Earth Planet. Sci. Lett.*, **95**, 114-122, 1987.
- Jager, E., W. J. Chen, A. J. Hurford, R. X. Liu, J. C. Hunziker, and D. M. Li, BB-6: A Quaternary age standard for K-Ar dating, *Chem. Geol.*, **52**, 275-279, 1985.
- Klein, E. M., and C. H. Langmuir, Ocean ridge basalt chemistry, axial depth, crustal thickness and temperature variations in the mantle, *J. Geophys. Res.*, **92**, 8089-8115, 1987.
- Krummenacher, D., and J. Noetzelin, Ages isotopiques K/Ar de roches prelevees dans les possessions francaises du Pacifique, *Bull. Soc. Geol. Fr.*, **8**, 173-175, 1966.
- Lacroix, A., Les roches alcalines de Tahiti, *Bull. Soc. Geol. Fr.*, **10**, 91-124, 1910.
- Lanphere, M. A., and F. A. Frey, Geochemical evolution of Kohala volcano, Hawaii, *Contrib. Mineral. Petrol.*, **95**, 100-113, 1987.
- Leotot, C., P.-Y. Gillot, F. Guichard, and R. Brousse, Le volcan de Taravao (Tahiti): un exemple de volcanisme polyphasique associe a une structure deffondrement. *Bull. Soc. Geol. Fr.*, **8**, 951-962, 1990.
- LeRoy, I., L. Turpin, H. Guillou, S. Chiesa, P.-Y. Gillot, and F. Guichard, Temporal evolution of the volcanism of Tahiti, 2, Geochemistry and isotopic compositions, paper presented at International Workshop on Intraplate Volcanism: The Polynesian Plume Province, August 2-7, Centre National de la Recherche Scientifique, Papeete, Tahiti, 1993.



- Levi, S., H. Audunsson, R. A. Duncan, L. Kristjansson, P.-Y. Gillot, and S. P. Jakobsson, Late Pleistocene geomagnetic excursion in Icelandic lavas: Confirmation of the Laschamp excursion, *Earth Planet. Sci. Lett.*, **96**, 443-457, 1988.
- Macdonald, G. A., and T. Katsura, Chemical composition of Hawaiian lavas, *J. Petrol.*, **8**, 82-133, 1964.
- Marshall, P., The geology of Tahiti, *Trans. Proc. N.Z. Inst.*, **47**, 361-377, 1915.
- McBirney, A. R., and K. Aoki, Petrology of the island of Tahiti, in *Studies in Volcanology: A Memoir in Honor of Howell Williams*, edited by R. R. Coats, R. L. Hay, and C. A. Anderson, *Mem. Geol. Soc. Am.*, **116**, 523-556, 1968.
- McNutt, M. K., and K. M. Fischer, The South Pacific superswell, in *Seamounts, Islands, and Atolls*, *Geophys. Monogr. Ser.*, vol. 43, edited by B. H. Keating, P. Fryer, R. Batiza, and G. W. Boehlert, pp. 25-34, AGU, Washington, D.C., 1987.
- Morgan, W. J., Convection plumes in the lower mantle, *Nature*, **230**, 42-43, 1971.
- Morgan, W. J., Deep mantle convection plumes and plate motions, *Am. Assoc. Pet. Geol. Bull.*, **56**, 203-213, 1972.
- Nakamura, N., Determination of REE, Ba, Fe, Mg, Na and K in carbonaceous and ordinary chondrites, *Geochim. Cosmochim. Acta*, **38**, 757-775, 1974.
- Natland, J. H., and D. L. Turner, Age progression and petrological development of Samoan shield volcanoes: Evidence from K-Ar ages, lava compositions, and mineral studies, in *Geological Investigations of the Northern Melanesian Borderland*, Circum-Pacific Council for Energy and Mineral Resources, *Earth Sci. Ser.*, vol. 3, edited by T. M. Brocher, pp. 139-171, Houston, Tex., 1985.
- Newsom, H. E., W. M. White, K. P. Jochum, and A. W. Hofmann, Siderophile and chalcophile element abundances in oceanic basalts, Pb isotope evolution and growth of the Earth's core, *Earth Planet. Sci. Lett.*, **80**, 299-313, 1986.
- Nielsen, R. L., Simulation of igneous differentiation processes, in *Modern Methods of Igneous Petrology: Understanding Magmatic Processes*, edited by J. Nicholls and J. K. Russell, *Rev. Mineral.*, **24**, 65-105, Mineralogical Society of America, Washington, D.C., 1990.
- Richards, M. A., B. H. Hager, and N. H. Sleep, Dynamically supported geoid highs over hotspots: Observation and theory, *J. Geophys. Res.*, **93**, 7690-7708, 1988.
- Roeder, P. L., and R. F. Emslie, Olivine-liquid equilibrium, *Contrib. Mineral. Petrol.*, **29**, 275-289, 1970.
- Sleep, N. H., Hotspots and mantle plumes: Some phenomenology, *J. Geophys. Res.*, **95**, 6715-6736, 1990.
- Stacey, F. D., and D. E. Loper, The thermal boundary layer interpretation of D'' and its role as a plume source, *Phys. Earth Planet. Inter.*, **33**, 45-55, 1983.
- Sun, S., and W. F. McDonough, Chemical and isotopic systematics of oceanic basalts: Implications for mantle composition and processes, in *Magmatism in the Ocean Basins*, edited by A. D. Saunders and M. J. Norry, Geological Society of London Spec. Pub. 42, London, pp. 313-345, 1989.
- Talandier, J., and E. Okal, The volcanoseismic swarms of 1981-1983 in the Tahiti-Mehetia area, French Polynesia, *J. Geophys. Res.*, **89**, 11,216-11,234, 1984.
- Tracy, R. J., Petrology and genetic significance of an ultramafic xenolith suite from Tahiti, *Earth Planet. Sci. Lett.*, **48**, 80-96, 1980.
- White, W. M., The sources of ocean basalts: Radiogenic isotopic evidence, *Geology*, **13**, 115-118, 1985.
- White, W. M., and A. W. Hofmann, Sr and Nd isotope geochemistry of oceanic basalts and mantle geochemistry, *Nature*, **296**, 821-825, 1982.
- White, W. M., M. M. Cheatham, and R. A. Duncan, Isotope geochemistry of Leg 115 basalts and inferences on the history of the Reunion mantle plume, *Proc. Ocean Drill Program, Sci Results*, v. 115, 53-61, 1990.
- White, W. M., J. M. Bird, K. S. Harpp, R. A. Duncan, R. Brousse, and T. Gisbert, Volcanic evolution of Tahaa: Does erosion cause post-erosional volcanism?, paper presented at International Workshop on Intraplate volcanism: The Polynesian Plume Province, August 2-7, Centre National de la Recherche Scientifique, Papeete, Tahiti, 1993.
- Williams, H., Geology of Tahiti, Moorea and Maïao, *Bull. 105*, 89 pp., B.P. Bishop Mus., Honolulu, HI, 1933.

---

R. A. Duncan, M. R. Fisk, and R. L. Nielsen, College of Oceanic and Atmospheric Sciences, Ocean Administration Building 104, Oregon State University, Corvallis, OR 97331. (email: rduncan@oce.orst.edu)

W. M. White, Department of Geological Sciences, Cornell University, Ithaca, NY 14853.

(Received November 22, 1993; revised April 5, 1994; accepted April 12, 1994.)